Polyhedron 30 (2011) 3026–3033

Contents lists available at ScienceDirect

Polyhedron

journal homepage: www.elsevier.com/locate/poly

The first non-acetato members of the bis(anion)octacarboxylatotetrakis{di-2-pyridyl-methanediolate(−2)}enneametal(II) family of complexes: Synthesis, X-ray structures and magnetism of $[M_9(N_3)_2(O_2CCMe_3)_8\{(py)_2CO_2\}_4]$ (M = Co, Ni)

Theocharis C. Stamatatos [a], Catherine P. Raptopoulou [b], Spyros P. Perlepes [a], Athanassios K. Boudalis [b,*]

[a] Department of Chemistry, University of Patras, 265 04 Patras, Greece
[b] Institute of Materials Science, NCSR "Demokritos", 153 10 Aghia Paraskevi Attikis, Greece

ARTICLE INFO

Article history:
Available online 20 February 2011

Keywords:
Cobalt(II) clusters
Nickel(II) clusters
Enneanuclearity
Di-2-pyridyl ketone
Crystal structures
Magnetic properties

ABSTRACT

The combined use of di-2-pyridyl ketone $[(py)_2CO]$ and azides (N_3^-) in nickel(II) and cobalt(II) pivalate chemistry has afforded complexes $[Ni_9(N_3)_2(O_2CCMe_3)_8\{(py)_2CO_2\}_4]$ (**1**) and $[Co_9(N_3)_2(O_2CCMe_3)_8\{(py)_2CO_2\}_4]$ (**2**), where $(py)_2CO_2^{2-}$ is the *gem*-diolate(−2) form of $(py)_2CO$. The complexes are isostructural and crystallize in the monoclinic $P2_1/c$ space group. Their molecular structures consist of nine metal(II) ions, eight of which are arranged as two parallel squares flanking the ninth. DC magnetic susceptometry on powdered samples of **1** (**1-p**) reveal an overall antiferromagnetic behavior, leading to an $S = 0$ ground state. AC susceptometry reveals out-of-phase signals between 10 and 27 K, and ZFC and FC experiments show a divergence of the two curves below ~27 K. Magnetization-decay and field-sweep experiments verify the relaxation behavior of the sample. Samples of the complex arising from carefully washed single crystals (**1-cr**) reveal a similar DC behavior, without however the appearance of cusps in the $\chi_M T$ versus T curves, and no relaxation. The relaxation behavior has been assigned to NiO impurities. The results illustrate the extreme care that should be taken when examining the magnetic properties of apparently analytically pure materials obtained under heating. Complex **2** exhibits an overall antiferromagnetic behavior, without observation of any relaxation phenomena.

1. Introduction

Molecular magnetism [1] is a rapidly growing field of interdisciplinary research whose central theme is the design, synthesis, characterization and study of molecular magnetic materials with tunable properties. Current trends [1b,2] in the field revolve around two main classes of molecular materials, *viz.*, multifunctional magnetic materials and molecular nanomagnets. The former holds promise for the realization of properties of technological interest previously thought to be possible only with atom-based inorganic solids, e.g., magnetic ordering combined with ferroelectricity, conductivity, or superconductivity. Families of materials that belong to this class are the switching magnetic materials (e.g., spin-crossover complexes [3] and magnets based on Prussian Blue analogues [4]) and the dual-function materials (e.g. ferromagnetic molecular metals [5]). The class of molecular nanomagnets [6] involves two families of compounds, single-molecule magnets (SMMs) [7] and single-chain magnets (SCMs) [8] which are essentially 1D analogues of SMMs.

SMMs are individual molecules capable of functioning as nanoscale magnetic particles and which thus represent a molecular approach to nanomagnetism. These materials combine the classic macroscale properties of a magnet with the quantum properties of a nanoscale entity. They display an impressive array of quantum effects that are observable up to higher and higher temperatures due to progress in molecular design, ranging from quantum tunneling of magnetization [9] to Berry phase interference [10] and quantum coherence [11] with important consequences on the physics of spintronic devices [12].

Generally speaking, SMMs require a ground state with a large magnetic moment and a high magnetic anisotropy. After 17 years of study, slow magnetization relaxation in transition-metal SMMs is rarely seen at temperatures above 2 K, and the highest blocking temperatures (below which slow relaxation is observed) remain at ~4.5 K [13]. Only Ln^{III} SMMs $[Ln(pc)_2]^-$ and $[Ln(pc)(pc^{\cdot})]$ (Ln^{III} = Tb^{III}, Dy^{III}, Ho^{III}; pc^- = phthalocyanine; $pc^{\cdot 2-}$ = oxidized phthalocyanine) [14–16] exhibit better performance, however these are also extremely rare examples.

Quite recently, the group of McInnes reported slow magnetization relaxation at 17 and 12 K in samples of symmetrical supertetrahedral Ni^{II}_{10} (**I**) [17] and Co^{II}_{10} (**II**) [18] clusters, respectively, i.e., at temperatures much higher than those for SMMs to date. Those

* Corresponding author. Tel.: +30 210 6503346; fax: +30 210 6503365.
E-mail address: tbou@ims.demokritos.gr (A.K. Boudalis).

0277-5387/$ - see front matter © 2011 Elsevier Ltd. All rights reserved.
doi:10.1016/j.poly.2011.02.025

exciting observations led the researchers to propose a quite different mechanism to account for slow relaxation in the absence of any significant energy barrier from either very high anisotropic spins (as in SMMs) or intermolecular interactions. The authors proposed [17,18] an unprecedented form of resonant phonon trapping to occur, leading to a breakdown of the heat-bath assumption for phonons.

The future of the 3d-metal cluster chemistry and the chances of identifying new SMMs or polynuclear metal complexes with interesting magnetic properties will both benefit from the development of new reaction systems or the refinement of old ones with suitable organic ligands. A modern trend is the use of two or even three ligands (combination of ligands or 'ligand blends') in the reaction systems. The loss of a degree of the synthetic control [19] is more than compensated for by the vast diversity of structural types using the combination of ligands. We have been exploring, amongst others [20], the ternary $(py)_2CO/R'CO_2^-/N_3^-$ ligand combination in 3d-metal chemistry as a source to high-nuclearity clusters, where $(py)_2CO$ is di-2-pyridyl ketone (Scheme 1). Studies with Mn [21], Fe [22], Co [23], Ni [24] and Cu [25] were fruitful and led to a great variety of high-spin molecules, some of which are SMMs [21,22]. The highly activated carbonyl group of $(py)_2CO$ makes this ligand special in modern coordination chemistry [26]. Water and alcohols (ROH), among other [27] nucleophiles, have been shown to add to the carbonyl group upon coordination of the carbonyl oxygen and/or the 2-pyridyl rings, generating the ligands $(py)_2C(OH)_2$ [the *gem*-diol form of $(py)_2CO$] and $(py)_2C(OR)(OH)$ [the hemiketal form of $(py)_2CO$], respectively (Scheme 1). Upon deprotonation, the latter becomes anionic $[(py)_2C(OR)O^-]$, whereas the former can function either as mono- $[(py)_2C(OH)O^-]$ or dianionic $[(py)_2CO_2^{2-}]$ depending on the reaction conditions. The great coordinative versatility and flexibility of the $(py)_2CO$-based anionic ligands [26] and the well known μ_2–μ_4 potential of the $R'CO_2^-$ and N_3^- [28] anions, had prompted us to combine the three ligand systems to aim for 3d-metal clusters. Our belief had been that the simultaneous employment of the three ligands in 1st-row transition metal chemistry would have given an extraordinary structural flexibility in the $(py)_2CO/R'CO_2^-/N_3^-$ mixed ligand system. This was, indeed, turned out to be the case [21–25].

Nine years ago we prepared and studied complexes $[M_9(N_3)_2(O_2CMe)_8\{(py)_2CO_2\}_4]$ (M^{II} = Co^{II} [23], Ni^{II} [24]) in which the nine M^{II} ions adopt a topology of two square pyramids sharing a common apex. Magnetic studies revealed ferromagnetic coupling mediated by the 4.40 azido bridges, giving a ground-state *S* value of 9 in the case of the Ni^{II}_9 cluster. This ground state total spin was further discussed by Shoji and coworkers [29] based on HDFT and DFT methods. Since the possibility of SMM behaviour was not examined for these clusters, we decided to go back to the general $M^{II}/(py)_2CO/R'CO_2^-/N_3^-$ reaction system and prepare analogues of the Ni^{II}_9 and Co^{II}_9 acetate clusters. We were interested in studying whether and how the nature of the carboxylate ligand affects the structural and magnetic identity of the product(s) resulting from this general reaction mixture.

Herein we report the preparation of the pivalate analogues of $[M_9(N_3)_2(O_2CMe)_8\{(py)_2CO_2\}_4]$ (M^{II} = Ni^{II}, Co^{II}), establishing the extension of this chemistry to other carboxylate ligands. Initial magnetic studies carried out on a powdered sample of the Ni^{II}_9 cluster (**1-p**) revealed some unexpected characteristics indicative of superparamagnetic behavior. These characteristics were absent in carefully washed single-crystalline samples of this complex (**1-cr**) and the Co^{II}_9 complex (**2**). The description of the static and dynamic magnetic properties of **1-p**, **1-cr** and **2** will be discussed and the probable origin of their behaviors will be presented.

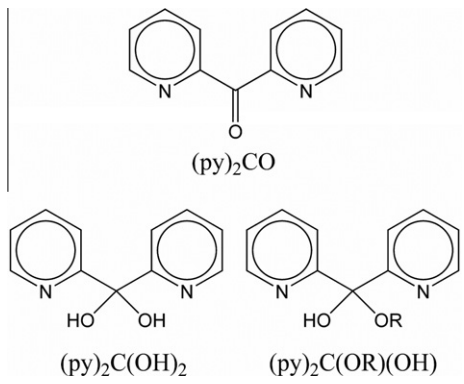

Scheme 1. The $(py)_2CO$-based ligands discussed in the text; note that $(py)_2C(OH)_2$, $(py)_2C(OR)(OH)$ and their anions exist only in their respective metal complexes (R = Me, Et, etc.).

2. Experimental

2.1. General and spectroscopic measurements

All manipulations were performed under aerobic conditions using materials as received. $[Ni_2(O_2CCMe_3)_4(HO_2CCMe_3)_4(H_2O)]$ [30] and $[Co_2(O_2CCMe_3)_4(HO_2CCMe_3)_4(H_2O)]$ [31] were prepared as described elsewhere. Caution! Although no such behavior was observed during the present work, azide salts are potentially explosive; such compounds should be synthesized and used in small quantities, and treated with utmost care at all times.

Elemental analyses for carbon, hydrogen, and nitrogen were performed on a Perkin–Elmer 2400/*II* automatic analyzer. Infrared spectra were recorded as KBr pellets in the range 4000–400 cm^{-1} on a Bruker Equinox 55/S FT-IR spectrometer. Variable-temperature magnetic susceptibility measurements were carried out on powdered samples in the 2–300 K temperature range using a Quantum Design MPMS SQUID susceptometer. Diamagnetic corrections for the complexes were estimated from Pascal's constants. Magnetization isotherms between 0 and 8 T (2 and 5 K) and AC magnetization experiments were carried out on a Quantum Design PPMS magnetometer. The energy levels stemming from the couplings among the Ni^{II} ions were calculated by employing the Kambe vector-coupling scheme to derive an analytical expression. The magnetic susceptibility of **1** was computed by using a routine to apply the van Vleck equation to the analytical expression previously determined. Least-squares fittings were accomplished with an adapted version of the function-minimization program MINUIT [32]. The error-factor *R* is defined as $R = \sum \frac{(\chi_{exp}-\chi_{calc})^2}{N\chi^2_{exp}}$ where *N* is the number of experimental points. Simulations of the magnetization *M* versus applied field *H* were carried out with the MAGPACK program package, using parameters derived from fits of the magnetic susceptibility [33].

2.2. Compound preparation

2.2.1. $[Ni_9(N_3)_2(O_2CCMe_3)_8\{(py)_2CO_2\}_4]$ (**1**)

Solid $[Ni_2(O_2CCMe_3)_4(HO_2CCMe_3)_4(H_2O)]$ (0.190 g, 0.20 mmol) and NaN_3 (0.013 g, 0.20 mmol) were added to a stirred, pale yellow solution of $(py)_2CO$ (0.036 g, 0.20 mmol) in DMF (25 mL). The resulting pale green solution was stirred under reflux for 2 h, during which time all the solids dissolved and the color of the solution changed to olive green. The solution was allowed to cool down at room temperature, filtered, and Me_2CO (50 mL) diffused into the filtrate. After several days, X-ray quality green prismatic crystals of **1**·Me_2CO appeared and were collected by filtration, washed with cold DMF (2 × 2 mL) and Me_2CO (2 × 3 mL), and dried under vacuum; the yield was 55% (0.054 g; based on the Ni^{II} starting

material). The dried solid analyzed as solvent-free (**1-p**). *Anal.* Calc. for $C_{84}H_{104}N_{14}O_{24}Ni_9$ (2223.93): C, 45.40; H, 4.72; N, 8.82. Found: C, 45.55; H, 4.59; N, 8.72%. IR data (KBr, cm^{-1}): 2953 (s), 2921 (m), 2862 (m), 2088 (vs), 1590 (vs), 1482 (s), 1423 (s), 1374 (m), 1357 (m), 1294 (m), 1231 (s), 1152 (m), 1125 (m), 1090 (m), 1037 (m), 977 (m), 898 (m), 804 (m), 776 (m), 752 (m), 691 (m), 648 (m), 610 (m), 600 (w), 480 (m), 443 (m), 420 (m).

*Preparation of sample **1-cr**.* The mother liquor of **1** was filtered on a filter paper, except for a minimum quantity required to keep the crystals of **1** immersed. A portion of the filtrate was added to the crystals, the mixture was vigorously shaken and the solvent was removed with a pipette. This procedure was repeated several times (using the other portions of the filtrate), so as to remove any powdered material that had been coprecipitated with the crystals. A quantity of such obtained single crystals was filtered on a filter paper and dried under vacuum, while another quantity was pipetted into an NMR tube with some drops of the mother liquor, and the tube was then flame sealed. The vacuum-dried samples gave repeatedly excellent analytical results. The sealed NMR tube was mounted to a plastic straw for measurements on the SQUID and PPMS magnetometers.

2.2.2. $[Co_9(N_3)_2(O_2CCMe_3)_8\{(py)_2CO_2\}_4]$ (**2**)

This complex was prepared in the same manner as complex **1** but using $[Co_2(O_2CCMe_3)_4(HO_2CCMe_3)_4(H_2O)]$ (0.190 g, 0.20 mmol) in place of $[Ni_2(O_2CCMe_3)_4(HO_2CCMe_3)_4(H_2O)]$. After several days, X-ray quality purple prismatic crystals of **2**·Me_2CO appeared and were collected as previously; the yield was 50% (0.049 g; based on the Co^{II} starting material). The dried solid analyzed as solvent-free. *Anal.* Calc. for $C_{84}H_{104}N_{14}O_{24}Co_9$ (2224.17): C, 45.36; H, 4.71; N, 8.82. Found: C, 45.50; H, 4.54; N, 8.73%. The IR spectrum of **2** was identical with that of **1**.

2.3. Single-crystal X-ray crystallography

A purple crystal of **2**·Me_2CO with approximate dimensions $0.20 \times 0.30 \times 0.50$ mm was mounted in a capillary. Diffraction measurements were made on a Crystal Logic Dual Goniometer diffractometer using graphite monochromated Mo radiation. Unit cell dimensions were determined and refined by using the angular settings of 25 automatically centered reflections in the range $11 < 2\theta < 23°$. Intensity data were recorded using a $\theta - 2\theta$ scan. Three standard reflections monitored every 97 reflections showed less than 3% variation and no decay. Lorentz, polarization and Ψ-scan absorption corrections were applied using CRYSTAL LOGIC software. The structure was solved by direct methods using SHELXS-97 [34] and refined by full-matrix least-squares techniques on F^2 with SHELXL-97 [35]. Further experimental crystallographic details for **2**·Me_2CO: $2\theta_{max} = 48°$; $(\Delta/\sigma)_{max} = 0.002$; $(\Delta\rho)_{max}/(\Delta\rho)_{min} = 0.571/-0.306$ e/Å^3. Hydrogen atoms of the $(py)_2CO_2^{2-}$ ligands were introduced at calculated positions as riding on bonded atoms. All non-hydrogen atoms were refined anisotropically. Most of the methyl groups of the pivalate ligands were found disordered and were refined over two positions with occupation factors summing one; no H-atoms for the pivalate ligands and the acetone solvate molecule were included in the refinement. Unit cell parameters and structure solution and refinement data for **2**·Me_2CO are listed in Table 1.

A green crystal of **1**·Me_2CO was similarly mounted in a capillary. Unit-cell determination [monoclinic, $P2_1/c$, $a = 25.126(16)$ Å, $b = 20.915(14)$ Å, $c = 21.124(13)$ Å, $\beta = 99.898(15)°$, $V = 10936(12)$ Å^3, $Z = 4$] revealed that the complex is isostructural to **2**·Me_2CO. Refinement of a partial dataset [R_1 and wR_2 values for observed data were 0.1152 and 0.2412, respectively] confirmed its identical connectivity, so data collection was not completed.

Table 1
Crystallographic data for **2**·Me_2CO.

Parameter	**2**·Me_2CO
Formula[a]	$C_{87}H_{110}Co_9N_{14}O_{25}$
Formula weight (g mol^{-1})[a]	2282.26
Crystal system	monoclinic
Space group	$P2_1/c$
T (K)	298(2)
λ (Å)	0.71073
a (Å)	25.164(7)
b (Å)	21.030(6)
c (Å)	21.264(5)
β (°)	100.590(11)
V (Å^3)	11061(5)
Z	4
ρ_{calc} (g cm^{-3})	1.370
μ (mm^{-1})	1.383
Reflections measured/unique	17345/16850 ($R_{int} = 0.0138$)
Reflections observed [$I > 2\sigma(I)$]	12949
Parameters refined	1360
R_1, wR_2[b] (all)	0.0691, 0.1436
R_1, wR_2[b] (obs.)	0.0468, 0.1292

[a] Including solvate molecules.
[b] $w = 1/[\sigma^2(F_o^2)+(aP)^2 + bP]$ and $P = (\max)F_o^2, 0) + 2F_c^2)/3$ ($a = 0.0703$, $b = 10.177$); $R_1 = \Sigma(|F_o| - |F_c|)/\Sigma(|F_o|)$ and $wR_2 = \{\Sigma[w(F_o^2 - F_c^2)^2]/\Sigma[w(F_o^2)^2]\}^{1/2}$.

3. Results and discussion

3.1. Synthetic comments and IR spectra

Two routes have been used for the preparation of complexes $[M^{II}_9(N_3)_2(O_2CMe)_8\{(py)_2CO_2\}_4]$ (M = Fe [22], Co [23], Ni [24]). The first approach is based on an "one-pot" procedure and requires the reaction of the divalent metal acetate, $(py)_2CO$ and NaN_3 in MeCN or DMF under reflux, see Eq. (1). The second approach [36] uses the hydroxo-bridged clusters $[M^{II}_9(OH)_2(O_2CMe)_8\{(py)_2CO_2\}_4]$ (M = Fe [22], Co [23], Ni [24]) as starting materials; the M^{II}_9/OH^- clusters react with a slight excess of N_3^- ions in DMF or DMF/MeOH to yield the desired azido-bridged clusters according to Eq. (2). This reaction scheme represents an example of a general synthetic route for the preparation of high-spin molecules [36]; it is based on the replacement of hydroxo bridges that most often propagate antiferromagnetic exchange interactions by the end-on azido ligand, which is a strong ferromagnetic coupler [28].

$$9M(O_2CMe)_2 \cdot xH_2O + 4(py)_2CO + 2NaN_3 \rightarrow [M_9(N_3)_2(O_2CMe)_8\{(py)_2CO_2\}_4] + 8MeCO_2H + 2NaO_2CMe + (9x-4)H_2O \quad (1)$$

$$[M_9(OH)_2(O_2CMe)_8\{(py)_2CO_2\}_4] + 2NaN_3 \rightarrow [M_9(N_3)_2(O_2CMe)_8\{(py)_2CO_2\}_4] + 2NaOH \quad (2)$$

Complex **1** was prepared using $[Ni_2(O_2CCMe_3)_4(HO_2CCMe_3)_4(H_2O)]$ [30] as starting material; this dinuclear complex is an ideal reagent for the preparation of Ni^{II} pivalate clusters [30]. The reaction of $[Ni_2(O_2CCMe_3)_4(HO_2CCMe_3)_4(H_2O)]$, $(py)_2CO$ and NaN_3 in an 1:1:1 molar ratio in DMF gave an olive green solution which upon layering with Me_2CO gave **1** in good yield; its formation is summarized in Eq. (3). The Ni^{II}-mediated nucleophilic attack of H_2O (mainly from the solvent) on the carbonyl group of $(py)_2CO$ is responsible for the formation of the *gem*-diolate(−2) ligand $(py)_2CO_2^{2-}$. The deprotonation of "$(py)_2C(OH)_2$" is achieved solely by the strongly basic pivalate groups. The reactants' molar ratio could be varied over a wide range and still gave **1**, although the 1:1:1 ratio gave the highest yield and most crystalline product. The stoichiometric $(py)_2CO:N_3^-$ ratio of 2:1, however, gave lower yields (~30%).

$$9[Ni_2(O_2CCMe_3)_4(HO_2CCMe_3)_4(H_2O)] + 8(py)_2CO + 4NaN_3 \rightarrow 2[Ni_9(N_3)_2(O_2CCMe_3)_8\{(py)_2CO_2\}_4] + 52HO_2CCMe_3 + 4NaO_2CCMe_3 + H_2O \quad (3)$$

The same procedure with $[Co_2(O_2CCMe_3)_4(HO_2CCMe_3)_4(H_2O)]$ [31] instead of $[Ni_2(O_2CCMe_3)_4(HO_2CCMe_3)_4(H_2O)]$ gave the isostructural complex $[Co_9(N_3)_2(O_2CCMe_3)_8\{(py)_2CO_2\}_4]$ (**2**) in good (~50%) yields.

The identical IR spectra of **1** and **2** do not exhibit a band in the region of the carbonyl stretching vibration [ν(CO)] as expected, with the nearest band at 1590 cm^{-1} assigned to a 2-pyridyl stretching vibration [this band also has a $\nu_{as}(CO_2)$ character] raised from 1582 cm^{-1} on coordination, as observed earlier [37] upon complex formation involving hydration of $(py)_2CO$. The complex exhibits an intense band at 2088 cm^{-1} assigned to the asymmetric stretching mode of the azido ligand [38]. The strong bands at 1590 and 1423 cm^{-1} are assigned to the $\nu_{as}(CO_2)$ and $\nu_s(CO_2)$ modes, respectively; the former should also involve a ring stretching character. The difference Δ [$\Delta = \nu_{as}(CO_2) - \nu_s(CO_2)$] is small (167 cm^{-1}), as expected for the bidentate bridging mode of carboxylate ligation [39].

3.2. Description of structures

The structures of **1** and **2** (Fig. 1) are very similar to those of the other complexes of the $[M_9(N_3)_2(O_2CMe)_8\{(py)_2CO_2\}_4]$ family [22–24], so they will not be described in detail. Briefly, we may report that they consist of two M^{II}_4 squares stacked parallel to each other in a slightly staggered conformation at a ~4.8 Å distance from each other, with a ninth M^{II} ion between them. The $(py)_2CO_2^{2-}$ dianion bridges five metal ions with the simultaneous formation of three chelating rings per ligand (coordination mode $\eta^1:\eta^3:\eta^3:\eta^1:\mu_5$). Each of the two end-on azides bridges four metal ions and caps the base of each M_5 square pyramid. Each M···M edge of the bases of the two pyramids is further bridged by one *syn*, *syn* $\eta^1:\eta^1:\mu_2$ pivalate. A salient feature of the structures is the coordination number of 8 for the central metal ion [Ni(1), Co(1)] which is extremely rare in Ni^{II} and Co^{II} chemistries. The chromophore of this metal ion is $M^{II}O_8$, the eight oxygen atoms coming from the four $(py)_2CO_2^{2-}$ ligands. The M^{II}_9 molecules are well separated from each other, due to the bulky pivalate groups on their peripheries. The central ions [Ni(1) and Co(1)] are ~14.8 Å from their closest symmetry counterparts, while the shortest $M^{II}\cdots M^{II}$ intermolecular distances are ~10.3 Å.

3.3. Magnetic properties of the Ni^{II} complex

The first sample of **1** that was examined was a powdered sample derived from filtration of the initially precipitated crystalline material (**1-p**). This sample had given very good analytical results (see Section 2). Its unexpected magnetic behavior (*vide infra*) prompted us to collect additional magnetic data from samples of single crystals of **1**, carefully isolated from their mother liquor and washed to remove eventual impurities (**1-cr**). Due to the collapse of the crystals upon evaporation of the lattice solvent molecules, the sample **1-cr** was studied (i) in a flame-sealed NMR tube, as single-crystals immersed in their mother liquor, and (ii) as a dried powder. These combined studies allowed us to verify that drying does not affect the chemical identity of **1-cr** and also to quantify these measurements by allowing us to obtain the sample's mass in the case of the dried powder. The data for **1-p** and for the dried **1-cr** sample are shown in Fig. 2.

3.3.1. Static magnetic susceptibility properties of *1-p*

The $\chi_M T$ product of **1-p** is 10.67 $cm^3\ mol^{-1}\ K$ (1 T), lower than the value predicted for nine non-interacting $S = 1$ ions (11.40 $cm^3\ mol^{-1}\ K$, $g = 2.25$). This is attributed to intramolecular antiferromagnetic interactions. This conclusion is corroborated by the constant decrease of $\chi_M T$ upon cooling, down to a value of 0.63 $cm^3\ mol^{-1}\ K$ at 2 K. This behavior is field-dependent below ~45 K. Under a 0.1 T field, the $\chi_M T$ decrease continues until a local minimum of 8.67 $cm^3\ mol^{-1}\ K$ at 38 K. Then, there is a small increase to a maximum of 9.87 $cm^3\ mol^{-1}\ K$ at 26 K, and finally, upon further cooling, $\chi_M T$ drops abruptly to a value of 0.96 $cm^3\ mol^{-1}\ K$ at 2 K. This peak disappears upon application of a 1 T field. Extrapolation of the $\chi_M T$ curve at $T = 0$ yields a $\chi_M T$ value of zero, suggesting an $S = 0$ ground state.

For the quantitative interpretation of the magnetic susceptibility data we assumed three different exchange interactions (Scheme 2), one along the edges of the square bases (J_1), one between the central Ni(1) and the external Ni^{II} ions (J_2) and an interaction along the diagonals of the square bases (J_3). The spin Hamiltonian for such a system is given by Eq. (4).

$$\hat{H} = -2J_1(\hat{S}_2\hat{S}_3 + \hat{S}_3\hat{S}_4 + \hat{S}_4\hat{S}_5 + \hat{S}_5\hat{S}_2 + \hat{S}_6\hat{S}_7 + \hat{S}_7\hat{S}_8 + \hat{S}_8\hat{S}_9 + \hat{S}_9\hat{S}_6) - 2J_2(\hat{S}_1\hat{S}_2 + \hat{S}_1\hat{S}_3 + \hat{S}_1\hat{S}_4 + \hat{S}_1\hat{S}_5 + \hat{S}_1\hat{S}_6 + \hat{S}_1\hat{S}_7 + \hat{S}_1\hat{S}_8 + \hat{S}_1\hat{S}_9) - 2J_3(\hat{S}_2\hat{S}_4 + \hat{S}_3\hat{S}_5 + \hat{S}_6\hat{S}_8 + \hat{S}_7\hat{S}_9) \quad (4)$$

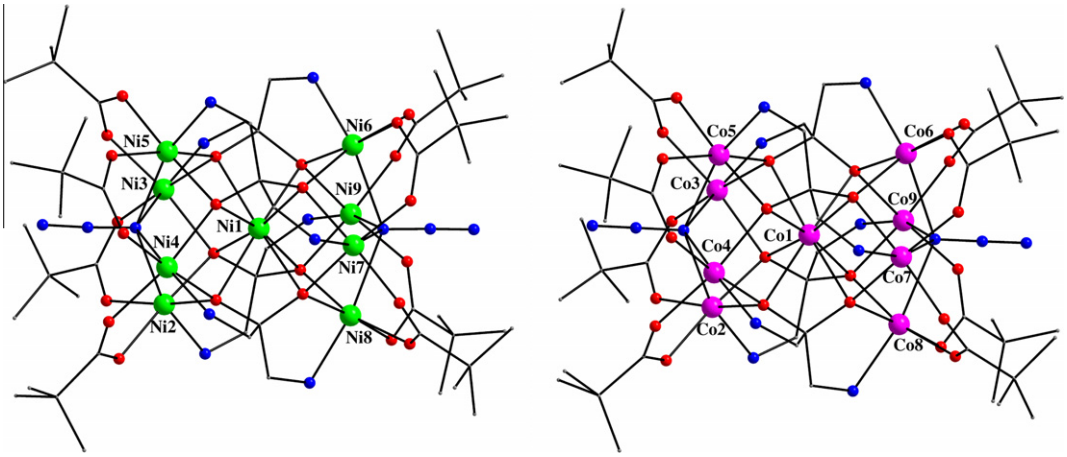

Fig. 1. Partially labeled POV-Ray plots of complexes **1** (left) and **2** (right). All H atoms and all non-coordinated atoms of the $(py)_2CO_2^{2-}$ ligands are omitted for clarity. Color scheme: Ni^{II}, green; Co^{II}, purple; O, red; N, blue; C, grey. (For interpretation of the references to colour in this figure legend, the reader is referred to the web version of this article.)

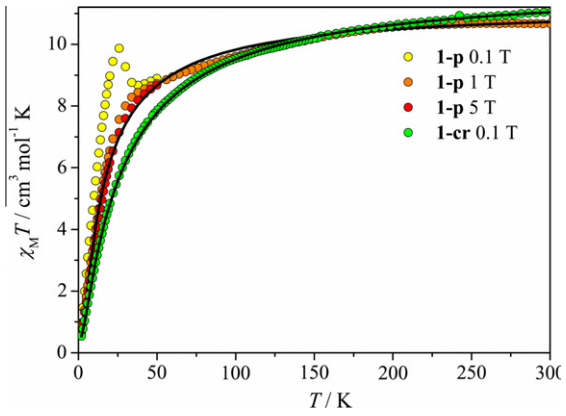

Fig. 2. $\chi_M T$ versus T curves for samples **1-p** and dried **1-cr** at various fields. Fits to the data of **1-p** (1 T) and **1-cr** (0.1 T) have been carried out as described in the text.

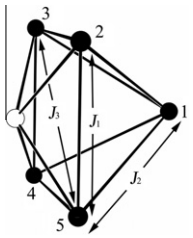

Scheme 2. Spin-coupling scheme used for the interpretation of the magnetic susceptibility data of **1**. The other half of the molecule is omitted for clarity.

Owing to the symmetry of the system, the Kambe vector-coupling approach [40] yielded the analytical expression for the energy levels presented in Eq. (5),

$$\begin{aligned} E_{(S_A,S_B,S_C,S_D,S_E,S_F,S_G,S_T)} = {} & J_1[S_A(S_A+1)+S_B(S_B+1)+S_C(S_C+1) \\ & +S_D(S_D+1)-S_E(S_E+1)-S_F(S_F+1)] \\ & +J_2[S_G(S_G+1)-S_T(S_T+1)]-J_3[S_A(S_A+1) \\ & +S_B(S_B+1)+S_C(S_C+1)+S_D(S_D+1)] \end{aligned} \quad (5)$$

where $\hat{S}_A=\hat{S}_2+\hat{S}_4, \hat{S}_B=\hat{S}_3+\hat{S}_5, \hat{S}_C=\hat{S}_6+\hat{S}_8, \hat{S}_D=\hat{S}_7+\hat{S}_9, \hat{S}_E=\hat{S}_A+\hat{S}_B, \hat{S}_F=\hat{S}_C+\hat{S}_D, \hat{S}_G=\hat{S}_E+\hat{S}_F$ and $\hat{S}_T=\hat{S}_1+\hat{S}_G$.

Data of **1-p** collected under very weak fields could not be fitted, due to relaxation phenomena explained below. It was therefore decided to fit the 1 T data. Fits over the 2–300 K temperature range yielded the best-fit parameters $J_1 = 1.1\ cm^{-1}$, $J_2 = -3.4\ cm^{-1}$, $J_3 = -6.5\ cm^{-1}$, $g = 2.23$ ($R = 5.4 \times 10^{-4}$), corresponding to a quadruply degenerate $S = 0$ ground state (with a non-degenerate first excited $S = 1$ state at $0.68\ cm^{-1}$).

3.3.2. Dynamic magnetic properties of *1-p*

To probe eventual relaxation phenomena in **1-p**, AC magnetic susceptibility experiments were carried out at various frequencies between 2 and 300 K. Unexpectedly, out-of-phase (χ''_M) signals were detected between 10 and 27 K (Fig. 3). These signals consist of two peaks, a broader one centered around 19 K and a narrower one at 25 K. The positions of these peaks show small frequency dependence over the frequency range tested (10^2–10^4 Hz).

Zero-field-cooled (ZFC) and field-cooled (FC) experiments under 0.01 and 0.1 T fields (Fig. S1) revealed that the χ_M versus T curves diverge below ~26 K, with the FC curves appearing above the ZFC ones. The phenomenon is field-dependent, with the divergence being much more pronounced at weak fields (0.01 T) than at stronger fields (0.1 T). Another interesting finding of these experiments was the fact that while the FC curves showed a single maximum,

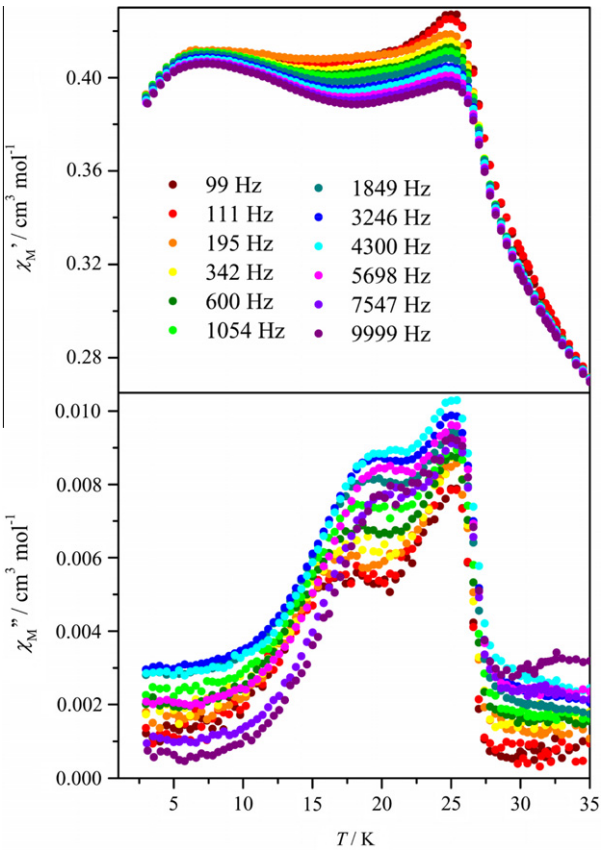

Fig. 3. χ'_M and χ''_M versus T data for sample **1-p** collected under oscillating fields of varying frequencies.

the ZFC curves showed more features. In particular, the 0.01 T curve exhibited two maxima at ~7 and ~21.5 K, while a shoulder centered around 14 K was also observed.

Magnetization decay experiments as a function of time for **1-p** (Fig. S2) revealed a slow decrease of the M/M_0 fraction at low temperatures. This was slowest at 2 K, accelerating at higher temperatures. Between 5 and 10 K the decrease remained practically constant, while it accelerated above 15 K. This quasiexponential decay could not be fitted to a single relaxation time, probably indicating a more complex relaxation process. Field-sweep experiments carried out between ±1 T at 2 K revealed a small but discernible hysteresis of ~550 G (Fig. S3). The width of this loop should be evaluated by considering the experimental limitations of our SQUID apparatus, which requires ~10 min to complete the ±1 T cycle.

3.3.3. Static magnetic susceptibility properties of *1-cr*

At this point we decided to assess the origin of these relaxation phenomena. The phenomenology of the behavior of **1-p** was very similar to that reported by Leznoff and coworkers [41], who observed slow magnetic relaxation around 20 K in samples of the coordination polymer $K\{Ni[Au(CN)_2]_3\}$. In particular, a sample of this material prepared under hydrothermal conditions (125 °C) exhibited a peak in its $\chi_M T$ versus T curve at 20 K, a divergence of its ZFC–FC curves, also at 20 K, and frequency-independent out-of-phase signals at 20.5 K. The fact that samples of the same material, prepared under non-hydrothermal conditions, exhibited simple paramagnetism and none of these effects, was attributed to the presence of NiO impurities observed by Tunneling Electron Microscopy.

It is generally considered that while NiO is an antiferromagnet ($T_N = 525$ K), NiO nanoparticles with average diameters of 3 and

7 nm behave as superparamagnets [42]. However, recent studies on NiO nanoparticles prepared by sol–gel methods, have shown these do not behave as superparamagnets, but rather as a spin glass due to surface spin disorder [43]. Such a behavior would agree with the frequency dependence of the out-of-phase signals of **1-p**; the ratio $\Delta T_f/[T_f\Delta(\log f)]$ (where T_f is the freezing temperature and f the frequency of the experiment) was ~0.057 for the low-temperature peak and ~0.014 for the high-temperature one, in agreement with a spin-glass behaviour.

Regardless of the origin of the magnetic relaxation, we concluded that this might be attributed to some impurity. With this in mind we proceeded to measure samples arising *exclusively* from single crystals of **1** (samples **1-cr**) to verify whether these unexpected results were indeed due to the cluster itself, or to an impurity. The 300 K $\chi_M T$ value of the dried portion of **1-cr** (11.04 $cm^3\ mol^{-1}$ K at 0.1 T) is close to that of **1-p**, but it decreases monotonously upon cooling, without exhibiting a peak, reaching a value of 0.53 $cm^3\ mol^{-1}$ K at 2 K (Fig. 2). Similarly to **1-p**, extrapolation of its $\chi_M T$ curve at $T = 0$ yields a $\chi_M T$ value of zero, suggesting an $S = 0$ ground state. The portion of **1-cr**, consisting of single crystals in a sealed NMR tube with drops of mother liquor, exhibits the same behavior.

The same model described above for **1-p** was employed for the interpretation of the data of the dried sample of **1-cr**, yielding two best-fit solutions with parameters $J_1 = 5.0\ cm^{-1}$, $J_2 = -8.5\ cm^{-1}$, $J_3 = -14.5\ cm^{-1}$, $g = 2.31$ ($R = 8.7 \times 10^{-5}$, solution **A**) and $J_1 = -3.5\ cm^{-1}$, $J_2 = -3.4\ cm^{-1}$, $J_3 = -6.3\ cm^{-1}$, $g = 2.30$ ($R = 4.6 \times 10^{-5}$, solution **B**). Both solutions **A** and **B**, like that of the data for **1-p**, correspond to quadruply degenerate $S = 0$ ground states with low-lying $S = 1$ excited states at 1.9 and 1.1 cm^{-1}, respectively. However, the quality of these fits was much superior to that of the fits of the data for **1-p**.

These results suggest that the dynamic behavior of **1-p** is not due to intrinsic properties of complex **1**, but probably due to the presence of NiO impurities. Although we did not proceed to identify those impurities, we note that the observed behavior is consistent with the one described for NiO nanoparticles, the formation of which is enhanced at higher reaction temperatures [41]. We must also note that we did not endeavor to determine the mechanism behind the magnetic relaxation phenomena of those impurities (i.e. spin-glas versus superparamagnetism), as this falls beyond the scope of the present work.

3.3.4. Magnetization studies

Isothermal magnetization curves collected at 2 and 5 K were similar for both samples **1-p** (shown in Fig. 4) and **1-cr**. These do not exhibit the onset of saturation even at 8 T, suggesting that the ground state is not well isolated. The magnetization M increases almost linearly with the magnetic field H at low fields (~1 T) but then shows a broad step centered around 4 T. The sigmoidal nature of the curve (as revealed by its derivative) indicates the successive population of excited states of higher spin multiplicities with increasing magnetic fields.

In order to verify the findings from the fits to the magnetic susceptibility data, we conducted simulations of the magnetization isotherms, using the best-fit parameters from these fits (Fig. 4). No data set offered an ideal simulation to the experimental data; this was not surprising, considering that magnetic susceptibility fits were carried out on single-field data, neglecting single-ion zero-field splitting contributions of Ni^{II} ions. However, from the simulations it was revealed that solution **A** reproduces better the features of the experimental curve, in particular its almost linear increase at low fields and its stepped feature at higher fields. The parameters from solution **B** lead to a less satisfactory simulation, exhibiting the onset of saturation at high fields. It is thus concluded

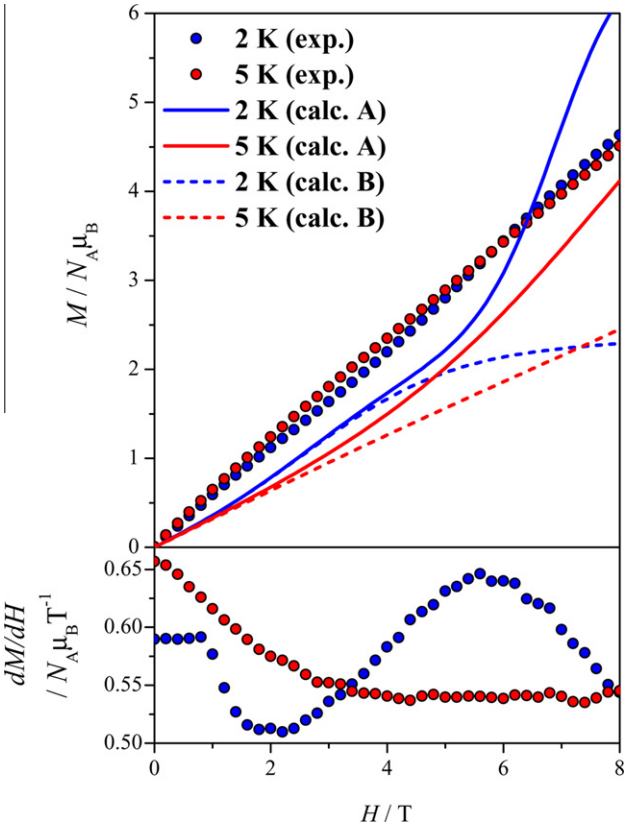

Fig. 4. Magnetization isotherms of **1-p** at 2 and 5 K (top) and their derivatives (bottom). Data for **1-cr** are similar. Simulations according to fits to the magnetic susceptibility data are shown for 2 K (solid lines) and 5 K (dashed lines).

that despite a higher agreement factor, R, solution **A** is the one best describing variable-temperature and variable-field data.

3.3.5. Discussion of the magnetic properties of *1*

The first observation that can be made concerns the comparison of the magnetic behaviors between complex **1** and its acetate analogue previously reported [24]; the acetate complex is ferromagnetic, exhibiting an $S = 9$ ground state, whereas complex **1** exhibits an $S = 0$ ground state.

From a structural perspective, key structural parameters are very similar between **1** and the acetate analogue; these are the Ni–N_{azido}–Ni angles along the sides of the rectangles (82.6–84.3° versus 84.1°, respectively) and the diagonals (139.8–141.5° versus 142.6°, respectively), and Ni–N_{azide} distances (2.293–2.398 Å versus 2.310 Å, respectively). The Ni–N_{azido}–Ni angles in **1** are slightly more acute, although it is difficult to quantify the effect of so small differences on magnetic exchange. A point of interest is that complex **1** exhibits a ferromagnetic interaction between the Ni^{II} ions bridged by end-on azides, as is generally expected for this bridging type, and also theoretically predicted for the acetate analogue [24]. However, due to the complicated spin-coupling scheme which causes densely packed magnetic spectra, subtle variations of the relative J_1, J_2 and J_3 values may have critical repercussions on the magnetic properties, resulting in smaller than expected ground-state S values.

Actually, Shoji et al. [29] previously conducted DFT calculations to explain the magnetic behavior of the acetate complexes $[Ni_9(X)_2(O_2CMe)_8\{(py)_2CO_2\}_4]$ ($X^- = OH^-$, N_3^-) and the influence exerted by the X^- ligands. They concluded that even though the ground state obtained using the calculated J values (no experimental J values are available [24]) may well agree with the experimen-

tal $S = 9$ state [24], fitting of the J values to the experimental magnetic data also indicates the possibility of a weak antiferromagnetic interaction between the Ni^{II} ions at the square-base diagonals, leading to an $S = 1$ ground state [29]. Such large ground-state variations were ascribed precisely to the existence of a multitude of low-lying magnetic states, each of which can be stabilized by a suitable magnetic field.

Finally, as to the reasons leading to J-value variations, apart from the strictly structural factors, we should not neglect the possible role of the carboxylate ligands. It is well known [44] that small changes in the peripheral ligand shell can modify the magnitude of exchange constants, but also can affect the overall magnetic behaviour, without causing discernible structural variations. We have previously observed in the series of the diferric clusters $[Fe_2O(O_2CR)_2(phen)_2(H_2O)_2](ClO_4)_2$ (R = H, CH_2F, CMe_3, CCl_3) [45], that variation of R induces electronic changes within the metal core, which alter the magnetic exchange couplings and Mössbauer parameters. Additional theoretical studies concerning the influence of the carboxylate ligands on the magnetic properties of the Ni^{II}_9 clusters would be very useful for the deep understanding of this system.

3.3.6. Magnetic properties of **2**

Magnetic susceptibility data for complex **2** are shown in Fig. 5. The $\chi_M T$ product is 24.93 $cm^3\ mol^{-1}\ K$ (1 T), higher than the value predicted for nine non-interacting $S = 3/2$ ions (16.88 $cm^3\ mol^{-1}\ K$, $g = 2$). This is assigned to the orbital contributions of the high-spin Co^{II} ions in octahedral environments to the magnetism. The $\chi_M T$ product decreases upon cooling, down to a plateau of 20.14 $cm^3\ mol^{-1}\ K$ at ~20 K, before decreasing rapidly upon further cooling (9.05 $cm^3\ mol^{-1}\ K$ at 2 K). This behavior is field-dependent below ~30 K. Under a 0.1 T field, the plateau is more pronounced, while it practically disappears at a field of 2.5 T. This behavior indicates dominant antiferromagnetic interactions, although a quantitative analysis is not undertaken due to the complications arising from the orbital contributions of high-spin Co^{II}.

With the small plateau being reminiscent of the magnetic behavior of **1**, we thought that the studied sample of complex **2** might also exhibit similar dynamic properties. However, AC susceptibility experiments carried out over a broad range of frequencies (100–10000 Hz) and temperatures (2–300 K) revealed no discernible out-of-phase signals, thus precluding the possibility of slow magnetic relaxation.

As in the case of **1**, complex **2** also shows remarkable differences in its magnetic behavior compared with that of its Co^{II}_9-acetate counterpart [23]. Although the acetate complex exhibits a similar $\chi_M T$ value at 300 K (23.38 $cm^3\ mol^{-1}\ K$), this value increases to a maximum of 25.29 $cm^3\ mol^{-1}\ K$ at 16 K, after passing through a broad and shallow minimum around 116 K. Again, this indicates possible electronic effects of the carboxylate alkyl group on magnetic exchange and is an issue deserving further theoretical study.

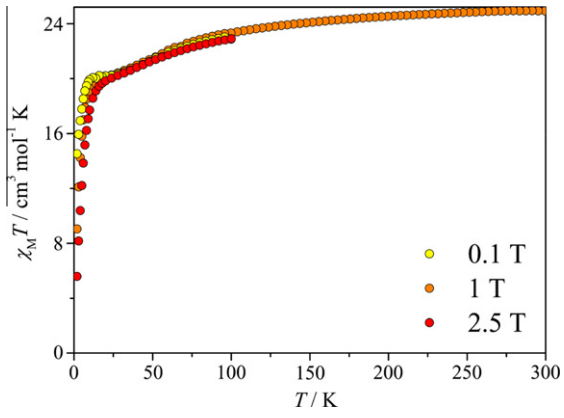

Fig. 5. $\chi_M T$ versus T data for **2** at various magnetic fields.

4. Concluding comments and perspectives

From a chemical perspective, the present results reveal general synthetic trends in the system $M^{II}/(py)_2CO/R'CO_2^-$. In particular they suggest that enneanuclear clusters of the family $[M_9(X)_2\{(py)_2CO_2\}_4(O_2CR')_8]$ exhibit a particular stability, which seems independent of the nature of the metal ion (M^{II} = Fe^{II}, Co^{II}, Ni^{II}), the monatomic bridge (X^- = OH^-, N_3^-, NCO^-), or the carboxylate ligand (R = Me, CMe_3). It rather seems that the $[M_9\{(py)_2CO_2\}_4]^{10+}$ unit is highly stable, permitting the replacement of its peripheral carboxylate "components" and inorganic monoatomic bridges without loss of the unit structure. This finding is of particular significance because it allows for additional synthetic modifications to extend this family of complexes. Most importantly, it is the addition of the carboxylate ligand as an extra degree of synthetic freedom that opens the most new synthetic vistas to many possible new members to this family, due to the large number of available variations.

From a magnetic perspective, this study is an indication that carboxylate ligands are "non-innocent" in the development of magnetic interactions. The – at first glance – trivial replacement of acetates by pivalates has led to a very different magnetic behavior.

Another important "lesson" from this work is that great care should be taken in the study of samples prepared at relatively high temperatures, because trace amounts of nanoparticulate impurities may also be generated. Such small amounts of magnetic nanoparticle impurities are sufficient to have a huge impact on the measured magnetic properties illustrating the shortcoming of conventional analytical methods, such as IR spectroscopy and elemental analysis. The danger of erroneously explaining the observed magnetic properties as due to the "pure" bulk material (clusters in our case) cannot thus be underestimated.

Acknowledgements

Th. C.S. and S.P.P. thank the European Social Fund (ESF), Operational Program for Educational and Vocational Training II (EPEAEK II), and particularly the Program PYTHAGORAS (Grant b.365.037), for funding the above work. We thank Dr. Juan-Modesto Clemente Juan for providing us with the code to fit the magnetic susceptibility data and Drs. Michael Pissas and Yiannis Sanakis for helpful discussions.

Appendix A. Supplementary data

CCDC 803804 and 803805 contains the supplementary crystallographic data for **1**·Me_2CO and **2**·Me_2CO. These data can be obtained free of charge via http://www.ccdc.cam.ac.uk/conts/retrieving.html, or from the Cambridge Crystallographic Data Centre, 12 Union Road, Cambridge CB2 1EZ, UK; fax: (+44) 1223-336-033; or e-mail: deposit@ccdc.cam.ac.uk. Supplementary data associated with this article can be found, in the online version, at doi:10.1016/j.poly.2011.02.025.

References

[1] (a) O. Kahn, Molecular Magnetism, VCH Publishers, New York, 1993;
(b) D. Gatteschi, L. Bogani, A. Cornia, M. Mannini, L. Sorace, R. Sessoli, Solid State Sci. 10 (2008) 1701.
[2] (a) E. Coronado, K.R. Dunbar, Inorg. Chem. 48 (2009) 3293 (preface for the Forum of this journal on Molecular Magnetism);

(b) M. Verdaguer, D. Gatteschi, C.R. Chimie 11 (2008) 1083 (foreword for the special issue of this journal concerning new trends in Molecular Magnetism).
[3] A.B. Gaspar, V. Ksenofontov, M. Seredyuk, P. Gütlich, Coord. Chem. Rev. 249 (2005) 2661.
[4] (a) O. Sato, T. Iyoda, A. Fujishima, K. Hashimoto, Science 272 (1996) 704;
(b) A. Bleuzen, C. Lomenech, V. Escax, F. Villain, F. Varret, C. Cartier, M. Verdaguer, J. Am. Chem. Soc. 122 (2000) 6648;
(c) E. Coronado, M.C. Gimenez-Lopez, T. Korzeniak, G. Vevchenko, F.M. Romero, A. Segura, V. Garcia-Baonza, J.C. Cezar, F.M. de Groot, A. Milner, M.J. Paz-Pasternak, J. Am. Chem. Soc. 130 (2008) 15519.
[5] E. Coronado, J.R. Galán-Mascaros, C.J. Gomez-Garcia, V.L. Lauhkin, Nature (London) 408 (2000) 447.
[6] D. Gatteschi, R. Sessoli, J. Villain, Molecular Nanomagnets, Oxford University Press, Oxford, UK, 2006.
[7] (a) For excellent reviews, see: R. Bagai, G. Christou, Chem. Soc. Rev. 38 (2009) 1011 (Tutorial Review);
(b) M. Murrie, D.J. Price, Annu. Rep. Prog. Chem., Sect. A 103 (2007) 20;
(c) G. Aromi, E.K. Brechin, Struct. Bond. 122 (2006) 1;
(d) R. Bircher, G. Chaboussant, C. Dobe, H. Güdel, S.T. Ochsenbein, A. Sieber, O. Waldman, Adv. Funct. Mater. 16 (2006) 209;
(e) D. Gatteschi, R. Sessoli, Angew. Chem., Int. Ed. 42 (2003) 268;
(f) J.R. Long, in: P. Yang (Ed.), Chemistry of Nanostructured Materials, World Scientific Publishing, Hong Kong, 2003, pp. 291–315;
(g) G. Christou, D. Gatteschi, D.N. Hendrickson, R. Sessoli, MRS Bull. 25 (2000) 66.
[8] (a) L. Bogani, A. Vindigni, R. Sessoli, D. Gatteschi, J. Mater. Chem. 18 (2008) 4750;
(b) C. Coulon, H. Miyasaka, R. Clérac, Struct. Bond. 122 (2006) 163;
(c) A. Caneschi, D. Gatteschi, N. Lalioti, C. Sangregorio, R. Sessoli, A. Venturi, A. Vindigni, A. Rettori, M.G. Pini, M.A. Novak, Angew. Chem., Int. Ed. 40 (2001) 1760.
[9] (a) J.R. Friedman, M.P. Sarachik, J. Tejada, R. Ziolo, Phys. Rev. Lett. 76 (1996) 3830;
(b) L. Thomas, F. Lionti, R. Ballou, D. Gatteschi, R. Sessoli, B. Barbara, Nature (London) 383 (1996) 145;
(c) C. Sangregorio, T. Ohm, C. Paulsen, R. Sessoli, D. Gatteschi, Phys. Rev. Lett. 78 (1997) 4645.
[10] (a) A. Garg, Europhys. Lett. 22 (1993) 205;
(b) W. Wernsdorfer, R. Sessoli, Science 284 (1999) 133;
(c) W. Wernsdorfer, M. Soler, G. Christou, D.N. Hendrickson, J. Appl. Phys. 91 (2002) 7164;
(d) W. Wernsdorfer, N.E. Chakov, G. Christou, Phys. Rev. Lett. 95 (2005) 037203.
[11] (a) A. Ardavan, O. Rival, J.J.L. Morton, S.J. Blundell, A.M. Tyryshkin, G.A. Timco, R.E.P. Winpenny, Phys. Rev. Lett. 98 (2007) 057201;
(b) S. Bertaina, S. Gambarelli, T. Mitra, B. Tsukerblat, A. Müller, B. Barbara, Nature (London) 453 (2008) 203.
[12] L. Bogani, W. Wernsdorfer, Nat. Mater. 7 (2008) 179.
[13] C.J. Milios, A. Vinslava, W. Wernsdorfer, S. Moggach, S. Parsons, S.P. Perlepes, G. Christou, E.K. Brechin, J. Am. Chem. Soc. 129 (2007) 2754.
[14] N. Ishikawa, M. Sugita, T. Ishikawa, S. Koshihara, Y. Kaizu, J. Am. Chem. Soc. 125 (2003) 8694.
[15] N. Ishikawa, M. Sugita, N. Tanaka, T. Ishikawa, S.-Y. Koshihara, Y. Kaizu, Inorg. Chem. 43 (2004) 5498.
[16] N. Ishikawa, M. Sugita, W. Wernsdorfer, J. Am. Chem. Soc. 127 (2005) 3650.
[17] S. Carretta, P. Santini, G. Amoretti, M. Affronte, A. Candini, A. Ghirri, I.S. Tidmarch, R.H. Laye, R. Shaw, E.J.L. McInnes, Phys. Rev. Lett. 97 (2006) 207201.
[18] L. Lisnard, F. Tuna, A. Candini, M. Affronte, R.E.P. Winpenny, E.J.L. McInnes, Angew. Chem., Int. Ed. 47 (2008) 9695.
[19] R.E.P. Winpenny, J. Chem. Soc., Dalton Trans. (2002) 1.
[20] (a) A.K. Boudalis, M. Pissas, C.P. Raptopoulou, V. Psycharis, B. Abarca, R. Ballesteros, Inorg. Chem. 47 (2008) 10674;
(b) A.K. Boudalis, C.P. Raptopoulou, B. Abarca, R. Ballesteros, M. Chadlaoui, J.-P. Tuchagues, A. Terzis, Angew. Chem., Int. Ed. 45 (2006) 432.
[21] Th.C. Stamatatos, K.A. Abboud, W. Wernsdorfer, G. Christou, Angew. Chem., Int. Ed. 47 (2008) 6694.
[22] A.K. Boudalis, Y. Sanakis, J.M. Clemente-Juan, B. Donnadieu, V. Nastopoulos, A. Mari, Y. Coppel, J.-P. Tuchagues, S.P. Perlepes, Chem. Eur. J. 14 (2008) 2514.
[23] G.S. Papaefstathiou, S.P. Perlepes, A. Escuer, R. Vicente, M. Font-Bardia, X. Solans, Angew. Chem., Int. Ed. 40 (2001) 884.
[24] G.S. Papaefstathiou, A. Escuer, R. Vicente, M. Font-Bardia, X. Solans, S.P. Perlepes, Chem. Commun. (2001) 2414.
[25] (a) Th.C. Stamatatos, V. Tangoulis, C.P. Raptopoulou, A. Terzis, G.S. Papaefstathiou, S.P. Perlepes, Inorg. Chem. 47 (2008) 7969;
(b) Th.C. Stamatatos, J.C. Vlahopoulou, V. Tangoulis, C.P. Raptopoulou, A. Terzis, G.S. Papaefstathiou, S.P. Perlepes, Polyhedron 28 (2009) 1656.
[26] (a) For reviews, see: G.S. Papaefstathiou, S.P. Perlepes, Comments Inorg. Chem. 23 (2002) 249;
(b) Th.C. Stamatatos, C.G. Efthymiou, C.C. Stoumpos, S.P. Perlepes, Eur. J. Inorg. Chem. (2009) 3361 (Microreview).
[27] (a) For example, see: Y. Li, S. Xiang, T. Sheng, J. Zhang, S. Hu, R. Hu, R. Fu, X. Huang, X. Wu, Inorg. Chem. 45 (2006) 6577;
(b) B.F. Abrahams, T.A. Hudson, R. Robson, Chem. Eur. J. 12 (2006) 7095.
[28] For a review, see: A. Escuer, G. Aromi, Eur. J. Inorg. Chem. (2006) 4721 (Microreview).
[29] M. Shoji, K. Koizumi, T. Hamamoto, Y. Kitagawa, S. Yamanaka, M. Okumura, K. Yamaguchi, Chem. Phys. Lett. 421 (2006) 483.
[30] G. Aromi, A.R. Bell, M. Helliwell, J. Raftery, S.J. Teat, G.A. Timco, O. Roubeau, R.E.P. Winpenny, Chem. Eur. J. 9 (2003) 3024.
[31] G. Aromi, A.S. Batsanov, P. Christian, M. Helliwell, A. Parkin, S. Parsons, A.A. Smith, G.A. Timco, R.E.P. Winpenny, Chem. Eur. J. 9 (2003) 5142.
[32] F. James, M. Roos, Comput. Phys. Commun. 10 (1975) 345.
[33] (a) J.J. Borrás-Almenar, J.M. Clemente-Juan, E. Coronado, B.S. Tsukerblat, Inorg. Chem. 38 (1999) 6081;
(b) J.J. Borrás-Almenar, J.M. Clemente-Juan, E. Coronado, B.S. Tsukerblat, J. Comput. Chem. 22 (2001) 985.
[34] G.M. Sheldrick, SHELXS-97, Structure Solving Program, University of Göttingén, Germany, 1997.
[35] G.M. Sheldrick, SHELXL-97, Crystal Structure Refinement Program, University of Göttingén, Germany, 1997.
[36] G.S. Papaefstathiou, A.K. Boudalis, Th.C. Stamatatos, C.J. Milios, C.G. Efthymiou, C.P. Raptopoulou, A. Terzis, V. Psycharis, Y. Sanakis, R. Vicente, A. Escuer, J.-P. Tuchagues, S.P. Perlepes, Polyhedron 26 (2007) 2089.
[37] P.K. Byers, A.J. Canty, L.M. Engelhardt, J.M. Partick, A.H. White, J. Chem. Soc., Dalton Trans. (1985) 981.
[38] K. Nakamoto, Infrared and Raman Spectra of Inorganic and Coordination Compounds, fourth ed., Wiley, New York, 1986. p. 290.
[39] G.B. Deacon, R.J. Phillips, Coord. Chem. Rev. 33 (1980) 227.
[40] K. Kambe, J. Phys. Soc. Jpn. 5 (1950) 48.
[41] J. Lefebvre, S. Trudel, R.S. Hill, D.B. Leznoff, Chem. Eur. J. 14 (2008) 7156.
[42] M. Ghosk, A. Biswas, A. Sundaresan, C.N.R. Rao, J. Mater. Chem. 16 (2006) 106.
[43] S.D. Tiwari, K.P. Rajeev, Phys. Rev. B 72 (2005) 104433.
[44] F. Klöwer, Y. Lan, J. Nehrkorn, O. Waldmann, C.E. Anson, A.K. Powell, Chem. Eur. J. 15 (2009) 7413.
[45] A.K. Boudalis, Y. Sanakis, C.P. Raptopoulou, V. Psycharis, Inorg. Chim. Acta 360 (2007) 39.